Received Date: 14-Dec-2015

Revised Date: 22-Jul-2016

Accepted Date: 02-Aug-2016

Article Type: Articles

Final version received date : 27 -Aug- 2016

Running head: Taylor's laws in Hokkaido voles

**Title: Population dynamics, synchrony, and environmental quality of Hokkaido voles lead to temporal and spatial Taylor's laws**

Authors: Joel E. Cohen[1], Takashi Saitoh[2]

Affiliations:

[1] Laboratory of Populations, The Rockefeller University and Columbia University, 1230 York Ave., Box 20, New York, NY 10065-6399, USA; also Department of Statistics, Columbia University, and Department of Statistics, University of Chicago

[2] Field Science Center, Hokkaido University, North-11, West-10, Sapporo 060-0811, Japan

* Corresponding author:

Joel E. Cohen

Laboratory of Populations, The Rockefeller University and Columbia University, 1230 York Ave., Box 20, New York, NY 10065-6399, USA

Email cohen@rockefeller.edu,

Takashi Saitoh Email: tsaitoh@fsc.hokudai.ac.jp



**Abstract**

Taylor's law (TL) asserts that the variance in a species' population density is a power-law function of its mean population density: log(variance) = $a + b \times$ log(mean). TL is widely verified. We show here that empirical time series of density of the Hokkaido gray-sided vole, *Myodes rufocanus*, sampled 1962-1992 at 85 locations, satisfied temporal and spatial forms of TL. The slopes ($b \pm$ standard error) of the temporal and spatial TL were estimated to be $1.613 \pm 0.141$ and $1.430 \pm 0.132$, respectively. A previously verified autoregressive Gompertz model of the dynamics of these populations generated time series of density which reproduced the form of temporal and spatial TLs, but with slopes that were significantly steeper than the slopes estimated from data. The density-dependent components of the Gompertz model were essential for the temporal TL. Adding to the Gompertz model assumptions that populations with higher mean density have reduced variance of density-independent perturbations and that density-independent perturbations are spatially correlated among populations yielded simulated time series that satisfactorily reproduced the slopes from data. The slopes ($b \pm$ standard error) of the enhanced simulations were $1.619 \pm 0.199$ for temporal TL and $1.575 \pm 0.204$ for spatial TL.

**Key words: Autoregressive time series, Density dependence, Gompertz model, Rodents, Taylor's law, Voles, Synchrony, Spatial correlation, Population dynamics**



## Introduction

Taylor's law (TL, Taylor 1961) is one of the most widely verified empirical rules in ecology (Taylor 1986, Eisler et al. 2008). When applied to a single species, TL asserts that the variance in the population density is a power-law function of its mean population density. The power-law form of TL is written: variance = $a \times (\text{mean})^b$, $a > 0$. Equivalently,

$$\log(\text{variance}) = \log(a) + b \times \log(\text{mean}). \qquad \text{equation 1}$$

The value of $b$ (but not of $\log(a)$) is independent of the base of the logarithms, which we chose to be 10, and of the scale (e.g., individuals/$m^2$ vs. individuals/$km^2$) used to measure population density. Both $\log(a)$ and $b$ are estimated by some statistical fitting procedure.

In the temporal TL, the mean and variance are calculated over observations of population density at different times in a given location and one data point (log(temporal mean), log(temporal variance)) is plotted for each location. In the spatial TL, the mean and variance are calculated over observations of population density in different spatial locations and one data point (log(spatial mean), log(spatial variance)) is plotted for each time of observation.

Many theories and interpretations of TL have been proposed, but none has gained universal or even widespread acceptance. Major questions are: Why TL is so widely observed? What mechanisms or processes generate TL? What can be learned from the values of $a$ and $b$? Insufficient progress has been made in answering these questions in part because many previous empirical studies have verified TL without testing the details of any model that leads to TL, while detailed theoretical models that lead to TL have often lacked correspondingly detailed empirical verification of the processes assumed (see reviews by Taylor 1986 and Eisler et al. 2008). One exception (Cohen et al.

2013) showed that a stochastic multiplicative population growth model predicted a spatial TL and that long-term tree censuses in Black Rock Forest, New York, were compatible with the assumptions of the model and the estimated parameters of TL. Although spatial density-dependence has been examined in relation to TL (Taylor et al. 1978), we are not aware that the interaction with TL of temporal density-dependence or density-independence has been examined previously.

Here we show, first, that empirical time series of population density of a rodent species repeatedly surveyed at multiple locations satisfied temporal and spatial TLs and, second, that a Gompertz autoregressive time-series model, previously demonstrated to describe these populations well (Stenseth et al. 2003), predicted the form and (under additional assumptions) the empirically estimated slopes of the temporal and spatial TLs. This model represented temporally density-dependent as well as temporally density-independent population regulatory factors. The agreement between the predictions of the Gompertz model and the temporal TL depended primarily on the model's density-dependence with one-year lag. Adding assumptions of spatial correlation among the density-independent perturbations of the Gompertz model and effects of habitat quality on the variance of density-independent perturbations of the Gompertz model enabled the enhanced model to approximate well the empirically estimated slopes of the temporal and spatial TLs.

The species investigated here, the gray-sided vole [*Myodes rufocanus* (Sundevall, 1846)], was an economically important pest of tree plantations (Kaneko et al. 1998). Rodents are still very important pests for agricultural products in Asia (John 2014). Better understanding via TL of the relation between the mean and the variance of population density offers the possibility to improve the efficiency and precision of pest population estimation and control, as it has for insect pests of soybeans (Kogan et al. 1974, Bechinski and Pedigo 1981) and cotton (Wilson et al. 1989). Better understanding of TL also has important implications for conservation and the interaction between ecology and evolution (Pertoldi et al. 2014).

**Materials and methods**

*Study design and data*

Hokkaido is the northernmost island (41° 24–45° 31 N, 139° 46–145° 49 E) of Japan and covers 78,073 km$^2$. The geography of Hokkaido and the data collection have been described (Stenseth et al. 2003). The Forestry Agency of the Japanese Government has investigated vole populations since 1954 in Hokkaido forests covering (as of 1992) 28,400 km$^2$. Rodent surveys were carried out twice a year [spring (May or June) and fall (September or October)]. Here we analyzed $N$ = 85 time series of gray-sided vole populations in the fall covering $T$ = 31 years (1962–1992) in the central and northernmost part of Hokkaido (the Asahikawa Regional Office, Forestry Agency of the Japanese Government, Saitoh et al. 1997), because this regional office provided the longest data sets. Fall data represented better inter-annual fluctuations because they varied more than spring data.

A basic unit of the rodent survey was 150 trap-nights, which consisted of 50 snap traps set at 10 m intervals on 0.5 ha of land for three consecutive nights (Saitoh et al. 1997, 1998). We defined vole population density as the number of voles captured per 150 trap-nights. The raw data $M_{t,j}$, the total number of trapped voles in a ranger office which carried out the rodent survey on several plots (several 150 trap-nights), are presented as DataS1.zip Appendix 1 in a $T \times N$ matrix with $T$ = 31 rows, one for each year $t$ = 1962, 1964, …, 1992, and $N$ = 85 columns, $j$ = 1, 2, …, 85, one for each ranger office. The amount of trapping effort (trap-nights) is given in DataS1.zip Appendix 2. There were no missing values.

*Statistical procedures*

The traditional frequentist (or "Fisher") estimates of population density (per 150 trap nights) were (counts of voles $M_{t,j}$ in year $t$ at site $j$)/(number of trap nights in year $t$ at site $j$/150). All actual trapping efforts (actual number of trap nights) were ≥ 150 trap nights.

We then used WinBUGS version 1.4.3, freely available software (Spiegelhalter et al. 2003, http://www.mrc-bsu.cam.ac.uk/software/bugs/) for Bayesian analysis using Markov Chain Monte Carlo methods to produce Bayesian (or "Bayes") estimates of population density (per 150 trap nights) for each year and study site. These Bayes estimates take account of trapping effort and assume Poisson variation in actual counts, given an expected mean. In brief, Bayesian estimates adjust each frequentist estimate (usually very slightly) by "borrowing strength" from the distribution of the full array of data, often (as here) reducing the effects of outliers. The resulting Bayes population estimates are presented in DataS1.zip Appendix 3 in a $T \times N$ matrix $N_{t,j}$ with 31 rows, one for each year, and 85 columns, one for each study site. All $N_{t,j} > 0$.

We compared the "Fisher" and "Bayes" estimates of population density, site by site, year by year. For low counts, Fisher and Bayes agreed closely, but when the Fisher counts exceeded about 35 voles per 150 trap nights, Bayes counts tended to be slightly less than Fisher counts (Fig. S1(a)). The temporal mean of Fisher counts agreed very closely with the temporal mean of Bayes counts (Fig. S1(b)) and likewise for the spatial means (Fig. S1(c)). However, the estimates of the spatial and temporal variances from Bayes were systematically slightly lower than those from Fisher. Neither the Fisher nor the Bayes estimates takes account of possible differences in observability of voles at different sites or in different years.

Sample estimates of the variance are highly variable when, as here, the number of observations is limited. Therefore we accepted the Bayes estimates of mean and variance as more reliable and used them in all subsequent analyses. By providing the raw data on which Bayes estimates are based, we enable anyone to do independent analyses of the counts and sampling efforts.

*Gompertz model*

For each population $j$, using the Bayesian estimates of $N_{t,j}$ in $x_{t,j} = \log_e(N_{t,j}) = 2.302585 \times \log_{10}(N_{t,j})$, we calculated the temporal mean of $x_{t,j}$ , $= \left(\frac{1}{31}\right) \sum_{t=1962}^{1992} x_{t,j}$, which is the natural logarithm of the geometric mean over time of $N_{t,j}$, and then subtracted $\overline{x_j}$ from the time series of $x_{t,j}$

to get the centered time series $y_{t,j} = x_{t,j} - \overline{x_j}$ for population *j*. Thus $y_{t,j}$ is the natural logarithm of $N_{t,j}$ divided by the geometric mean over time of $N_{t,j}$. Then we fitted the Gompertz model, a homogeneous (no constant term) second-order autoregressive model to $y_{t,j}$:

$$y_{t,j} = (1+a_{1,j})y_{t-1,j} + a_{2,j}y_{t-2,j} + e_{t,j}, \qquad \text{equation 2}$$

where the *j*th population's coefficient of density dependence for a 1-year lag is $a_{1,j}$ and for a 2-year lag is $a_{2,j}$. The error term $e_{t,j}$ represents density-independent effects. It is modeled by a normal distribution with mean equal to 0 and a standard deviation $SD_j$ that is constant in time but may differ from one population *j* to another.

Instead of modeling process and observation separately, we used WinBUGS to obtain Bayesian estimates of $a_{1,j}$, $a_{2,j}$, and $SD_j$ taking sampling error into consideration (WinBUGS code is in DataS1.zip Appendix 5). The median of the posterior distribution was used for each parameter estimate. We also estimated those parameters using Yule-Walker estimation as coded in the 'aryule.m' function in the Signal Processing Toolbox of Matlab (MathWorks 2015) (results in DataS1.zip Appendix 3).

The Gompertz model (equation 2) can describe various fluctuation patterns of population dynamics (Royama 1992) and is commonly applied to analyses of vole populations (Saitoh et al. 1997, 1998, Stenseth et al. 1996, 1998). But the Gompertz model does not explicitly link $a_1$ and $a_2$ to underlying demographic processes of birth, death, and migration. Hence it is not yet possible to interpret $a_1$ and $a_2$ in terms of these processes. Despite numerous analyses of cyclic patterns in vole populations, how demographic processes control rodent population cycles remains hypothetical (Andreassen et al. 2013). While the rates of the reproduction and survival of Hokkaido voles are expected to be negatively affected by higher density, the relative importance of these demographic components of population change in explaining annual population fluctuations remains unclear. Quantitative information on the magnitudes and population-dynamic consequences of immigration and emigration is very limited.

Nevertheless, values of $a_1$ and $a_2$ can be interpreted, on a relative basis, in terms of ecological density dependence or density independence. Specifically, $a_1$ represents a return tendency to an equilibrium density (density dependence in a narrow sense) and populations with more negative values are less variable, while $a_2$ generates variability for a population and populations with more negative values are more likely to be cyclic (Royama 1992). Density dependence with a 1-year lag is strong and prevalent in populations of the Hokkaido vole (Saitoh et al. 1997, 1998, Stenseth et al. 2003).

*Simulations*

We generated three simulations using progressively stronger assumptions which were demanded by our progressively deeper understanding of the data: the so-called Fundamental simulations, the Adjusted SD simulations, and the Synchronized $e_t$ simulations. The state variable in all simulations was the centered log-transformed population density $y_{t,j} = x_{t,j} - \overline{x_j}$. The values of $y_{t,j}$ generated by each simulation were then transformed back to the original scale of population density using the observed temporal sample means $\overline{x_j}$, and then the means and variances that appear in the tests of TL were computed from these reverted values.

The Fundamental simulation used the Gompertz model (equation 2) with the population-specific estimates of $a_{1,j}$ and $a_{2,j}$ and $SD_j$ to generate 85 time series corresponding to 85 observed populations. The initial two observed centered log-transformed values $y_{1,j}$, $y_{2,j}$ were used for the first two values of each simulated population. The length of every simulated time series was 31 years, the same as observed.

We also did two additional simulations. The Adjusted SD simulations differed from the Fundamental simulation only in replacing $SD_j$ by the estimated $SD_j - 0.174 \times 2.302585 \times \log_{10}$(estimated temporal mean $\overline{x_j}$) for each $j$. The empirical basis for this adjustment is described in Results and its ecological rationale and interpretation are explained in the Discussion.

To generate the Synchronized $e_t$ simulations, we first generated a fixed "baseline error" time series $e_{t,0}$ of 31 independent and identically distributed normal random numbers with mean 0 and SD 1. Then we generated 85 correlated time series $e_{t,j}$, $j$ = 1, …, 85, of length 31 years ($t$ = 1, …, 31), using the formula $e_{t,j} = \rho \times e_{t,0} + (1 - \rho)^{1/2} \times \mathcal{N}_{t,j}(0, 1)$, where $\mathcal{N}_{t,j}(0, 1)$ are independent and identically distributed normal random numbers with mean 0 and SD 1. Consequently, the correlation over time between the error terms of any two simulated time series, for example, $e_{t,1}$ and $e_{t,2}$, would be $1 - \rho^2$ if the time series were infinitely long. We examined the effect of $\rho$ on the simulated spatial TL by an Approximate Bayesian Computation method (Csilléry et al. 2012). This procedure was a numerical search for the level of spatial correlation of population dynamics that gave the best agreement between the log(mean) and log(variance) of simulations and the log(mean) and log(variance) on the original scale of measurement of population density.

*Temporal Taylor's law*

For each population $j$ = 1, 2, …, 85, separately, we calculated the sample mean $\bar{N}_j = \left(\frac{1}{31}\right)\sum_{t=1962}^{1992} N_{t,j}$ of Bayesian estimated population density $N_{t,j}$ over time ("temporal sample mean") and the sample variance over time ("temporal sample variance") $\left(\frac{1}{30}\right)\sum_{t=1962}^{1992}\left(N_{t,j} - \bar{N}_j\right)^2$ of the $j$th time series of 31 Bayesian estimates of the number of voles per 150 trap-nights ($N_{t,j}$: $t$ = 1962, 1963, …, 1992) in R (DataS1.zip Appendix 3). We defined

$$X(\text{population } j) = \log_{10}(\text{temporal sample mean of } N_{t,j}),$$

$$Y(\text{population } j) = \log_{10}(\text{temporal sample variance of } N_{t,j}).$$

We used ordinary least-squares regression (OLS) to fit equation 1 to these 85 values of $X$(population $j$) and $Y$(population $j$). The use of OLS to fit log-log transformed versions of power laws has been criticized (Tokeshi 1995, Packard 2009, Packard et al. 2011). Strictly speaking, the use of OLS is invalid when observation errors are included in the abscissa, and here every observation of $X$(population $j$) is subject to sampling variability. However, the use

of OLS in fitting TL is recommended (Xiao et al. 2011, Lai et al. 2013) because the sampling variability of $X$(population $j$) is much smaller than the sampling variability of $Y$(population $j$), and numerous practical evaluations of using OLS to fit TL suggest that it gives reasonable results. Therefore we used OLS.

To test for nonlinearity in the relation between $Y$(population $j$) and $X$(population $j$), we used OLS to fit a quadratic generalization of TL (due to Taylor et al. 1978, their equation 14): $Y(\text{population } j) = \log(a) + b \times X(\text{population } j) + c \times [X(\text{population } j)]^2$. We accepted TL as an approximate representation of the relationship of temporal sample variance to temporal sample mean if $c$ in the quadratic model did not differ significantly from zero and the slope $b$ in the linear model, equation 1, differed significantly from zero.

All regressions were computed using function "lm" in R version 3.2.2. The critical value for statistical significance was always $P = 0.05$ without any correction for multiple inferences.

*Spatial Taylor's law*

For each year $t$ = 1962, 1963, …, 1992, separately, we calculated the sample mean $\overline{N_t} = \left(\frac{1}{85}\right)\sum_{j=1}^{85} N_{t,j}$ of Bayesian estimated population density $N_{t,j}$ ("spatial sample mean") and the sample variance $\left(\frac{1}{84}\right)\sum_{j=1}^{85}\left(N_{t,j} - \overline{N_t}\right)^2$ ("spatial sample variance") over the 85 populations $j$ = 1, …, 85 (DataS1.zip Appendix 3). We defined

$$X(\text{year } t) = \log_{10}(\text{spatial sample mean of } N_{t,j}),$$

$$Y(\text{year } t) = \log_{10}(\text{spatial sample variance of } N_{t,j}).$$

Using the same procedure as for the temporal TL, we fitted equation 1 and tested for nonlinearity by fitting a quadratic generalization of TL.

*Factors influencing Taylor's law*

The simulations of the Gompertz model are determined by three parameters ($a_1$, $a_2$, and SD) and the estimated mean of empirical densities. Since more negative $a_1$ represents a stronger force to return densities to equilibrium, higher values of $a_1$ are predicted to increase the variance of densities. Since populations with more negative values of $a_2$ are more likely to be cyclic (Royama 1992), higher values of $a_2$ are predicted to decrease the variance of densities. Since SD determines the degree of density-independent disturbance, higher values of SD are predicted to increase the variance of densities.

We analyzed the effects of the parameters of the Gompertz model on the variance and mean of the empirical and simulated densities by means of generalized linear model (GLM) analyses with the three parameters as explanatory variables and the log(variance) and log(mean) of empirical and simulated densities as separate response variables. If the Gompertz model sufficiently captured the population dynamics, the GLM analyses would be expected to yield similar results when comparing empirical and simulated time series.

In addition, if a parameter consistently affects both variance and mean, that parameter is considered to contribute to the formation of TL. For example, if a factor $X$ is linearly related to both log(variance) and log(mean), i.e., if $X$ satisfies log(variance) = $r + s\times X$ and log(mean) = $u + v\times X$, $v \neq 0$, then TL must be true. Why? Solving for $X$ in the second equation gives $X = [\log(\text{mean}) - u]/v$ and then the first equation gives $\log(\text{variance}) = r + s\times[\log(\text{mean}) - u]/v = (r - s\times u/v) + (s/v)\times\log(\text{mean})$. This linear relationship between log(variance) and log(mean) is TL with intercept $r - s\times u/v$ and slope $s/v$. If the signs of $s$ and $v$ are same (both are negative or positive), that factor $X$ contributes to forming a positive slope of TL. If the signs of $s$ and $v$ are different, that factor $X$ leads towards a negative slope of TL.

**Results**

*Basic features of population fluctuation*

Densities fluctuated with 2-5 year periods (Fig. 1[A]). In some years most populations showed a peak or a trough of density. For example, $\log_{10}$(densities) of 61 populations (71.8%) were lower than 0.5 in 1975, while those of 67 populations (78.8%) were higher than 1.0 in 1978. The range of $\log_{10}$ spatial mean densities was 0.273-1.316 for 85 populations. Like spatial mean densities, the $\log_{10}$ spatial variance of densities also fluctuated over time, ranging between 0.739 and 2.264. As a function of year $t$, the spatial means and spatial variances showed no pronounced or statistically significant trends (slope = -0.004, $t$ = -0.800, $P$ = 0.430, adjusted $R^2$ = -0.012 for the mean; slope = -0.004, $t$ = -0.510, $P$ = 0.614, adjusted $R^2$ = -0.025 for the variance).

The 85 observed populations were generally pairwise correlated over time but the extent (even the sign) of the correlation varied widely. The mean of the 3,570 pairwise correlation coefficients (3570 = 85 × 84/2) of population density measured by the Bayesian adjusted population density was 0.297 ± 0.202 (SD). The maximum pairwise correlation was 0.902 and the minimum was -0.378. The correlation coefficients were significantly higher than zero in 1392 pairs (39.0%).

A linear regression of the pairwise correlation on the $\log_{10}$ of pairwise Euclidean distance [range: 3645 – 226970 m] between each pair of populations had slope ± standard error = -0.228 ± 0.011 ($P \approx 2\times10^{-16}$) but the adjusted $R^2$ = 0.1071 was not high. These results indicate that nearer populations had more closely correlated population dynamics but other factors in addition to distance evidently affected the correlation of population dynamics.

*Temporal and spatial Taylor's laws*

We tested TL by using the Bayesian estimates $N_{t,j}$ of population density, *not* log-transformed and *not* centered, but on the original scale of measurement, to calculate the temporal and spatial variances and means.

TL described adequately the relation of *Y*(population *j*) = log(temporal variance) of population density to *X*(population *j*) = log(temporal mean) of population density (Fig. 1[B]), with slope *b* ± standard error = 1.613 ± 0.141 and adjusted $R^2$ = 0.607 (Table S1). Quadratic regression revealed no statistically significant evidence of nonlinearity.

TL described the relation of *Y*(year *t*) = log(spatial variance) of population density to *X*(year *t*) = log(spatial mean) of population density (Fig. 1[C]), with slope *b* ± standard error = 1.430 ± 0.132 and adjusted $R^2$ = 0.795 (Table S2), a tighter linear relationship than the temporal TL. Quadratic regression revealed no statistically significant evidence of nonlinearity.

*Do simulations of the Gompertz model obey a temporal Taylor's law?*

In the Fundamental simulations, log(temporal variance) of density was linearly related to log(temporal mean) of density (Fig. 2[A]) with slope *b* ± standard error = 2.699 ± 0.214 (Table S3). Quadratic regression revealed no statistically significant evidence of nonlinearity. In comparison with the observed populations, Fundamental simulated populations showed a significantly steeper slope of TL (Table S3; ANCOVA, $t$ = 4.054, $P << 0.001$). Although the log(temporal mean) of both observed populations and Fundamental simulations fell in the range from roughly 0.6 to 1.3 (that is, roughly 4 = $10^{0.6}$ to 20 = $10^{1.3}$ voles per 150 trap-nights), the log(temporal variance) of observed populations ranged from roughly 0.8 to 2.3 (Fig. 1[C]) while the log(temporal variance) of Fundamental simulations ranged from roughly 1.0 to 4.0 (Fig. 2[A]), a range twice as wide.

In GLM analyses of the effects of the Gompertz parameters on the temporal variance of densities, $a_1$ and SD showed positive effects on the temporal variance while $a_2$ had negative effects, for both the empirical and the Fundamental simulated densities, as predicted (Table 1). The effects of SD only (not $a_1$ and $a_2$) were statistically significant. In contrast, the GLM had very small, and statistically insignificant, adjusted $R^2$ for the model of the temporal mean of the empirical and Fundamental simulated densities, so the Gompertz parameters did not explain variations in the temporal mean, empirical or Fundamental simulated.

When SD (alone) was regressed on the empirical temporal mean densities, we found SD = 1.384 – 0.174 $\times$ $\log_e$(temporal mean), with $R^2$ = 0.043, $F_{1.83}$=4.743, $P$ = 0.032. Using this relationship between SD and the empirical temporal mean in the simulations, we adjusted SD using the following equation: Adjusted SD = estimated SD of the empirical densities – 0.174 $\times$ $\log_e$(temporal mean of empirical densities). For these Adjusted SD simulations, a clear linear relation was observed between log(temporal variance) of density and log(temporal mean) (Fig. 2D), and every parameter of the regression of the simulated log(temporal variance) as a function of the simulated log(temporal mean) was similar to that for the temporal TL for observed populations (for Adjusted SD simulations: slope $b$ ± standard error = 1.671 ± 0.321 and adjusted $R^2$ = 0.237; see also Table S4; ANCOVA, $P$ > 0.6). Both log(temporal mean) and log(temporal variance) of density showed good agreements between observed populations and the Adjusted SD simulations (Fig. 2[E and F], Table S4).

*Do simulations of the Gompertz model obey a spatial Taylor's law?*

Using exactly the same time series produced by Adjusted SD simulations that realistically approximated the temporal TL, we tested whether the Gompertz model could simulate the observed spatial TL (Fig. 1C). The simulated log(spatial variance) of density was a linear function of the simulated log(spatial mean) of density, with no significant evidence of nonlinearity (Table S5). The slope $b$ ± standard error = 3.283 ± 0.464 was significantly steeper than the slope of the observed TL (Table S5; ANCOVA, $t$ = 4.109, $P$ = 0.001).

The pairwise correlation over time of the 85 time series (corresponding to 85 spatial locations) produced by the Adjusted SD simulation was low, as expected, since independent error terms were used for each population and each year. The mean of the correlation coefficients, 0.013 ± 0.183 (SD), was significantly lower than the mean of the pairwise correlations of the observed 85 populations (*t*-test, $t = 40.050$, $P << 0.001$). The percentage of positive significant correlations for the Adjusted SD simulation (4.7%) was very close to the value expected by chance, as expected.

To examine whether the lack of spatial correlation in the Adjusted SD simulation might be responsible for the difference in the spatial TL between the observed populations and the Adjusted SD simulations, correlated time series were generated by using spatially (not temporally) correlated $e_{t,j}$ (Methods). When $\rho = 0.617$, the Synchronized $e_t$ simulations' time series produced a most likely set of time series that satisfied both TLs. The mean of the spatially pairwise correlations over time in the Synchronized $e_t$ simulations was 0.201, not so different from the mean of the spatially pairwise correlations over time in the observed populations (0.297). In the Synchronized $e_t$ simulations, the log(spatial variance) of density was linearly related to log(spatial mean) of density (Fig. 3[D]), with slope $b$ ± standard error = 1.575 ± 0.204. No significant differences were found in the slope and the intercept between the observed populations and the Synchronized $e_t$ simulations (Table S6; ANCOVA, $P >$ 0.5). However, the log(spatial mean) and log(spatial variance) of density did not show tight agreement between observed populations and the Synchronized $e_t$ simulations (Fig. 3[E and F]), Table S6). Quadratic regression did not show any statistically significant evidence of nonlinearity (Table S6) in the relation of the Synchronized $e_t$ simulated variance to the Synchronized $e_t$ simulated mean.

The Synchronized $e_t$ simulation also showed a clear temporal TL (Fig. 3[A]), with slope $b$ ± standard error = 1.619 ± 0.199. No significant differences were found in the slope and the intercept between the observed populations and the Synchronized $e_t$ simulations (Table S7; ANCOVA, $P > 0.4$). Both log(temporal mean) and log(temporal variance) of density showed relatively good agreements between observed populations and the Synchronized $e_t$ simulation (Fig. 3[B and C]), Table S7).

The same simulation analyses were carried out using the parameters estimated by the Yule-Walker method. They provided results resembling those from the Bayesian estimates. The Fundamental simulation provided the form of temporal and spatial TLs, but with slopes that were significantly steeper than the slopes estimated from the data (Table S8 - S12). The Synchronized $e_t$ simulation generated simulated time series that satisfied both the temporal TL with slope $b$ ± standard error = 1.794 ± 0.172 and the spatial TL with slope $b$ ± standard error = 1.540 ± 0.251 through the Adjusted SD simulation (Table S11 and S12, Fig. S2).

**Discussion**

*Empirical results on Taylor's law*

In populations of gray-sided voles surveyed at 85 sites in Hokkaido, Japan, from 1962 through 1992, the temporal variance (variance over time) of the Bayesian estimated population density was approximately a power law function of the temporal mean (mean over time). This finding illustrated the temporal TL. The slope of the log(variance)-log(mean) relationship was estimated to be $b$ ± standard error = 1.613 ± 0.141 (Table S1). The estimated density also satisfied a spatial TL. The slope was estimated to be $b$ ± standard error = 1.430 ± 0.132 (Table S2). There was no statistically significant evidence of nonlinearity in temporal or spatial relationships.

*Interpretation of the slope of Taylor's law*

The slope *b* of TL is not an indicator of the absolute level of variation in population density. Rather, *b* is an "elasticity," in economic jargon, that is, *b* is approximately the proportional rate of increase of the variance of population density associated with a given proportional increase in the mean of population density. For example, if *b* = 1.613, as in the observed temporal TL, and if a first population has temporal mean density that is 1% larger than that of a second population, so that $\overline{N_1} = 1.01 \times \overline{N_2}$, then, on average, the first population will have a temporal variance of population density very nearly (but not exactly) 1.613% larger than that of the second, because $Var(N_1) = a(\overline{N_1})^{1.613} = a(1.01 \times \overline{N_2})^{1.613} = 1.01^{1.613} \times a(\overline{N_2})^{1.613} \approx 1.01618 \times Var(N_2)$. In general, if $\epsilon$ is much smaller than 1 (in the example, $\epsilon = 0.01 \ll 1$), then $(1+\epsilon)^b \approx 1+b\epsilon$ so if the mean is increased by the factor $1+\epsilon$ or by $100\epsilon$%, then the variance is increased approximately by the factor $1+b\epsilon$ or by $100b\epsilon$%. The smaller $\epsilon$ is, the more accurate the approximation is.

The coefficient of variation is defined as the standard deviation divided by the mean. When TL has slope $0 < b < 2$, as for these vole populations, a population that is more abundant on average has a larger variance but smaller coefficient of variation.

*Simulations of the Gompertz model*

Previously, the population dynamics of gray-sided voles at the study sites had been shown to be described well by the Gompertz model (equation 2). In this linear autoregressive model, the dynamic variable was the logarithm of population density, and density dependence operated with one-year lags (quantified by parameter $a_1$) and two-year lags (quantified by parameter $a_2$). Density-independent random effects (quantified by parameter SD) were assumed independent in time and space but with standard deviations that varied from site to site.

The GLM model including all parameters of the Gompertz model ($a_1$, $a_2$, and SD) had significant ability to explain the variation of the variance of densities, but not variation in the mean of densities (Table 1). Since the estimated mean of an observed population was given as an equilibrium density to simulations, the mean of simulated densities was very probably influenced more by the estimated mean than by the three parameters of the Gompertz model. The parameters may have indirectly influenced the mean of simulated densities through influencing the variability of densities.

To investigate whether the Gompertz model could account for the observed temporal and spatial TLs, we performed three sets of simulations under differing assumptions. In all sets of simulations, log(temporal variance) was approximately a linear function of log(temporal mean), and log(spatial variance) was approximately a linear function of log(spatial mean), confirming that the Gompertz model could generate the *form* of a temporal and a spatial TL.

However, the temporal and spatial TLs in the Fundamental simulation were significantly steeper than the observed temporal and spatial TLs. The temporal TL slope of the Fundamental simulation (2.699 ± 0.214) was higher than 2. The slopes of TL that are commonly observed in many empirical examples lie between 1 and 2 (Taylor and Woiwod 1980). The slopes of the temporal and spatial TLs of the observed vole populations (1.613 ± 0.141 and 1.430 ± 0.132) were also included in this range.

*Modified simulations of the Gompertz model*

To make the Gompertz model's TLs have parameters that matched the parameters of the observed TLs, we incorporated two ecological effects, the heterogeneity of habitat quality and the synchrony of density independent factors. These simulations differed from the Fundamental simulations in two respects: the standard deviation of the density-independent error term was reduced by the equation of Adjusted $SD_j$ = estimated $SD_j - 0.174 \times \log_e$(estimated temporal mean) for each $j$, and the density-independent error term was spatially correlated with correlation $1 - \rho^2 = 1 - (0.617)^2 = 0.619$, resulting in an average (over pairs) value of the pairwise correlation between simulated time series of 0.201, not far from the observed average pairwise correlation of 0.297.

In Adjusted SD simulations, we assumed that populations in low-quality habitats have lower mean density but higher variability, whereas populations in high-quality habitats have higher mean density and lower variance of density. This assumption may be realistic. Population densities in low-quality habitats may usually be low but they sometimes become unusually high due to immigrants from a population in a high-quality habitat in outbreak years. Since differences in densities between usual and outbreak years may be higher in populations in low-quality habitats in comparison with those in high-quality habitats, the negative relationship between temporal mean and SD could realistically be expected.

The Adjusted SD simulations, which realistically approximated the temporal TL, reproduced the form of the spatial TL but implied a slope far larger than that of the observed spatial TL. In the Synchronized $e_t$ simulations, in which the density-independent error terms ($e_t$) in the Gompertz model were correlated across space (while retaining independence in time), every parameter of the regression of log(spatial variance) as a function of log(spatial mean) (in particular, $b$ ± standard error = 1.658 ± 0.141, Table S6) was similar to that for the observed spatial TL. In addition, the Synchronized $e_t$ simulations reproduced the temporal TL (Table S7), with simulated slope $b$ ± standard error = 1.596 ± 0.227. There was no statistically significant evidence of nonlinearity in the Synchronized $e_t$ simulations, nor of a difference in intercept or slope of a temporal TL between the Synchronized $e_t$ simulations and the observed populations.

*Interpretation of the modified simulations in terms of ecological mechanisms*

We interpreted the effects on the TL slope of the adjustments in the Synchronized $e_t$ simulations in terms of a simple simulation model that assumed some habitats were more favorable for vole population density than others. The details of this simulation are not presented here, as the model served for conceptual exploration rather than quantitative explanation. In this model, habitat heterogeneity was represented by the variation of carrying capacity. Each population grew following the logistic equation and fluctuated with stochastic effects. Movements occurred from a population

in a higher quality habitat (a source population) to a neighboring population in a lower quality habitat (a sink population) when the density of the population in the higher quality habitat exceeded its carrying capacity.

Simulations of this model generated the following results. When each population was independent, the spatial and the temporal slopes of TL were higher than 2, and therefore higher than observed. When density-dependent movements were introduced, the spatial and temporal slopes of TL were lowered to the interval between 1 and 2 of the observed spatial and temporal TL slopes.

We understand the effects of the assumptions of this model on the temporal TL as follows. Movements from a population in a higher-quality habitat to a population in a lower-quality habitat when the density of the population in a higher-quality habitat exceeded the carrying capacity reduced the temporal mean and variance of the populations in higher-quality habitats and enhanced the temporal mean and variance of the populations in lower-quality habitats. Since the absolute densities that were subtracted or added were equal, the relative densities added to the populations in lower-quality habitats were higher than those subtracted from the populations in higher-quality habitats. Thus the assumed population movements would be expected to lower the slope of the temporal TL.

We understand the effects of the assumptions of this model on the spatial TL as follows. Movements from a population in a higher-quality habitat to a population in a lower-quality habitat when the population density in a higher-quality habitat exceeded the carrying capacity reduced the densities of populations in higher-quality habitats and enhance the densities of populations in lower-quality habitats. Therefore, the spatial variance was reduced by the movements, whereas the spatial mean was not affected by the movement. In a year having higher spatial mean densities, populations in higher-quality habitat were prone to exceed their carrying capacity. As a result, the assumed population movements would be expected to lower the slope of the spatial TL.

This hypothesis has three strengths. First, it explains the milder slopes of the observed temporal and the spatial TL by a single, simple mechanism, namely, density-dependent movement in a source-sink dynamics system. Second, the concept of source-sink dynamics is well established. Demographic surpluses in higher-quality habitats (sources) and deficits in lower-quality habitats (sinks) commonly arise, and movement among local populations can stabilize dynamics at regional scales (Dias 1996; Heinrichs et al. 2016). Third, there is some evidence of density-dependent dispersal in voles, although this topic is controversial (Berthier et al. 2006).

*Future research questions*

We are not aware of mathematics that shows analytically that the Gompertz model with or without adjustments can generate temporal and spatial TLs, and we are not aware of explicit formulas that express the slopes and intercepts of the temporal and spatial TLs as explicit functions of the parameters of the correlated Gompertz model ($a_1$, $a_2$, SD, and ρ). Mathematical (by contrast with numerical) analysis of the relation between the Gompertz model, equation 2, and Taylor's law, equation 1, remains an open problem.

Since the Synchronized $e_t$ simulation showed good agreement with the observed TLs, we suggested that the heterogeneity of habitat quality and the synchrony of some density-independent factor lowered the spatial and temporal TL slope. This statement should be regarded as a hypothesis about nature for further empirical testing and mathematical analysis.

The success of the Synchronized $e_t$ simulations indicated that density dependence may be a driving force leading to the TLs. Since density dependence is the necessary and sufficient condition for sustainable populations (Royama 1992) and density dependence prevails in real populations (Brook and Bradshaw 2006), we suggest one possible answer to the question about why TL is so widely observed: sustainable populations may have a kind of density dependence that brings about TL. This suggested answer leads to further questions: why and how does some kind of density dependence form TLs, and what kinds of density dependence lead to TL?

The log(spatial mean) and log(spatial variance) of density did not agree well between the Synchronized $e_t$ simulations and the observed populations (Fig. 3[E and F]), even though the spatial TL, Fig. 3[D] (as well as the temporal TL, Fig. 3[A]) generated by the Synchronized $e_t$ simulations did agree well with the corresponding TLs of the data. Each data point in Fig. 3[E and F] is an average or a variance over 85 populations in one year. While we could estimate the magnitude of stochastic effects on each population's entire dynamics for the study period as SD, we could not predict or model temporal changes in stochastic effects (for example, why some years were peaks and some years were troughs). Therefore, the sequence of the degree of stochastic effects used in the simulations did not fit that for observed populations, and the spatial mean and variance of simulated populations differed from the observed ones. In future work, it would be of interest to examine whether meteorological or other environmental factors like sea surface temperature may play a causal role in the fluctuations of population density that we now treat as stochastic variability.

This study illustrates a scientific application of Taylor's laws that may be useful elsewhere, namely, using TLs as additional criteria to evaluate population-dynamic models. In this study, the previously verified Gompertz model could not reproduce quantitatively the empirically estimated slopes of the TLs. Taking account of habitat quality and synchrony accounted quantitatively for the slopes of observed TLs. In other cases where TLs are verified, testing whether population-dynamic models can account for them may lead to improved assumptions that help link Taylor's law to population dynamics.

**Acknowledgments**

T.S. thanks the Forestry Agency of Japanese Government for providing the data. Keiichi Fukaya and Hayato Iijima gave T.S. helpful advice for statistical analyses. J.E.C. thanks Priscilla K. Rogerson for assistance and U.S. National Science Foundation grant DMS-1225529 for partial support.

**Literature cited**

Andreassen, H. P., P. Glorvigen, A. Rémy, and R. A. Ims 2013. New views on how population-intrinsic and community-extrinsic processes interact during the vole population cycles. Oikos 122: 507–515.

Bechinski, E. J. and L. P. Pedigo. 1981. Population dispersion and development of sampling plans for *Orius insidiosus* and *Nabis* spp. in soybeans. Environmental Entomology 10:956-959.

Berthier, K., N. Charbonnel, M. Galan, Y. Chaval, and J. F. Cosson. 2006. Migration and recovery of the genetic diversity during the increasing density phase in cyclic vole populations. Molecular Ecology 15: 2665–2676.

Brook, B. W. and C. J. A. Bradshaw. 2006. Strength of evidence for density dependence in abundance time series of 1198 species. Ecology 87: 1445-1451.

Cohen, J. E., M. Xu, and W. S. F. Schuster. 2013. Stochastic multiplicative population growth predicts and interprets Taylor's power law of fluctuation scaling. Proceedings of the Royal Society Series B 280:20122955.

Csilléry, K., O. Francois, and M. G. B. Blum. 2012. abc: an R package for approximate Bayesian computation (ABC). Methods in Ecology and Evolution 3:475–479.

Dias, P. C. 1996. Sources and sinks in population biology. Trends in Ecology and Evolution 11:326-330.

Eisler, Z., I. Bartos, and J. Kertész. 2008. Fluctuation scaling in complex systems: Taylor's law and beyond. Advances in Physics 57:89-142.

Heinrichs, J. A., J. J. Lawler, and N. H. Schumaker. 2016. Intrinsic and extrinsic drivers of source-sink dynamics. Ecology and Evolution: 892–904.

John, A. 2014. Rodent outbreaks and rice pre-harvest losses in Southeast Asia. Food Security 6: 249-260.

Kaneko, Y., K. Nakata, T. Saitoh, N. C. Stenseth, and O. N. Bjørnstad. 1998. The biology of the vole *Clethrionomys rufocanus*: a review. Researches on Population Ecology 40: 21-37.

Kogan, M., W. G. Ruesink, and K. McDowell. 1974. Spatial and temporal distribution patterns of the bean leaf beetle, *Cerotoma trifurcata* (Forster), on soybeans in Illinois. Environmental Entomology 3:607-617.

Lai, J., B. Yang, D. Lin, A. J. Kerkhoff, and K. Ma. 2013. The allometry of coarse root biomass: log-transformed linear regression or nonlinear regression? PLoS ONE 8(10): e77007.

MathWorks (2015) MATLAB R2015a. Mathworks Inc., Natick, MA.

Packard, G. C. 2009. On the use of logarithmic transformations in allometric analyses. Journal of Theoretical Biology 257:515-518.

Packard, G. C., G. F. Birchard, and T. J. Boardman. 2011. Fitting statistical models in bivariate allometry. Biological Reviews 86:549-563.

Pertoldi, C., S. Faurby, D. H. Reed, J. Knape, M. Björklund, P. Lundberg, V. Kaitala, V. Loeschcke, and L. A. Bach. 2014. Scaling of the mean and variance of population dynamics under fluctuating regimes. Theory in Biosciences 133:165–173.

Royama, T. 1992. Analytical population dynamics. Chapman and Hall, London.

Saitoh, T., N. C. Stenseth, and O. N. Bjørnstad. 1997. Density dependence in fluctuating grey-sided vole populations. Journal of Animal Ecology 66: 14-24.

Saitoh, T., N. C. Stenseth, and O. N. Bjørnstad. 1998. Population dynamics of the vole *Clethrionomys rufocanus* in Hokkaido, Japan. Researches on Population Ecology 40: 61-76.

Spiegelhalter, D. J., A. Thoma, N. G. Best, and D. Lunn. 2003. WinBUGS user manual (version 1.4). MRC Biostatistics Unit, Institute of Public Health, Cambridge

Stenseth, N. C., O. N. Bjørnstad, and T. Saitoh. 1998. Seasonal forcing on the dynamics of *Clethrionomys rufocanus*: modeling geographic gradients in population dynamics. Researches on Population Ecology 40: 85-95

Stenseth, N. C., H. Viljugrein, T. Saitoh, T. F. Hansen, M. O. Kittilsen, E. Bølviken, and F. Glöckner. 2003. Seasonality, density dependence, and population cycles in Hokkaido voles. Proceedings of the National Academy of Sciences of the United States of America 100:11478-11483.

Taylor, L. R. 1961. Aggregation, variance and the mean. Nature 189:732–735.

Taylor, L. R., I. P. Woiwod, and J. N. Perry. 1978. The density-dependence of spatial behaviour and the rarity of randomness. Journal of Animal Ecology 47:383–406.

Taylor, L. R. and I. P. Woiwod. 1980. Temporal stability as a density dependent species characteristic. Journal of Animal Ecology 49: 209–224.

Taylor, L. R. 1986. Synoptic dynamics, migration and the Rothamsted insect survey: Presidential Address to the British Ecological Society, December 1984. Journal of Animal Ecology 55:1-38.

Tokeshi M. 1995. On the mathematical basis of the variance-mean power relationship. Researches on Population Ecology 37:43-48.

Wilson, L. T., W. L. Sterling, D. R. Rummel, and J. E. DeVay. 1989. Quantitative sampling principles in cotton. Pages 85-119 *in* R. E. Frisbie, K. M. El-Zik, and L. T. Wilson, editors. Integrated Pest Management Systems and Cotton Production. John Wiley & Sons, Inc., New York, USA.

Stenseth, N. C., O. N. Bjørnstad, and T. Saitoh. 1996. A gradient from stable to cyclic populations of *Clethrionomys rufocanus* in Hokkaido, Japan. Proceedings of Royal Society London B 263:1117-1126.

Xiao, X., E. P. White, M. B. Hooten, S. L. Durham. 2011. On the use of log-transformation vs. nonlinear regression for analyzing biological power laws. Ecology 92:1887-1894.

**Table**

Table 1. Partial regression coefficient estimates (PRC), standard error (SE), *t*-value, and standardized partial regression coefficients (β) of explanatory variables in the generalized linear model for temporal variance [temporal variance ~ direct density effect ($a_1$) + delayed density effect ($a_2$) + density independent effect (SD)] on (a) empirical densities and (b) simulated densities. Results on temporal mean [temporal mean ~ direct density effect ($a_1$) + delayed density effect ($a_2$) + density independent effect (SD)] are given in (c) for empirical densities and in (d) for simulated densities. The model fitting was assessed by adjusted $R^2$ and *F*-statistics. $^{*} < 0.05$, $^{**} < 0.01$, $^{***} < 0.001$.

| | (a) Variance of empirical densities | | | | (b) Variance of simulated densities | | | |
|---|---|---|---|---|---|---|---|---|
| parameter | PRC | SE | *t*-value | β | PRC | SE | *t*-value | β |
| $a_1$ | 0.191 | 0.191 | 0.191 | 0.191 | 0.191 | 0.191 | 0.191 | 0.191 |
| $a_2$ | -0.135 | -0.135 | -0.135 | -0.135 | -0.135 | -0.135 | -0.135 | -0.135 |
| SD | 0.291 | 0.291 | 0.291 | 0.291 | 0.291 | 0.291 | 0.291 | 0.291 |
| Intercept | 1.277 | 1.277 | 1.277 | 1.277 | 1.277 | 1.277 | 1.277 | 1.277 |
| | Adjusted $R^2$= 0.061 | | $F_{3,81}$= 2.839$^{*}$ | | Adjusted $R^2$= 0.311 | | $F_{3,81}$= 13.63$^{***}$ | |

| | (c) Mean of empirical densities | | | | (d) Mean of simulated densities | | | |
|---|---|---|---|---|---|---|---|---|
| parameter | PRC | SE | *t*-value | β | PRC | SE | *t*-value | β |
| $a_1$ | 0.082 | 0.065 | 1.152 | 0.142 | 0.046 | 0.078 | 0.595 | 0.069 |
| $a_2$ | -0.011 | 0.055 | -0.204 | -0.023 | -0.03 | 0.066 | -0.461 | -0.054 |
| SD | -0.135 | 0.063 | -2.162$^{*}$ | -0.233 | 0.114 | 0.749 | 1.519 | 0.167 |
| Intercept | 0.997 | 0.067 | 14.960$^{***}$ | – | 0.837 | 0.08 | 10.498$^{***}$ | – |
| | Adjusted $R^2$= 0.038 | | $F_{3,81}$= 2.114 | | Adjusted $R^2$= -0.0001 | | $F_{3,81}$= 0.996 | |

**Figure captions**

Fig. 1. (A) Observed time series of the $\log_{10}$ Bayesian estimate of population density $N_{t,j}$ of 85 gray-sided vole populations in Hokkaido, Japan in 1962, …, 1992. (B) Test of temporal TL for population density. The straight solid line is the least-squares linear regression of $\log_{10}$(temporal variance) as a function of $\log_{10}$(temporal mean) for observed populations. The curved dotted line is the least-squares quadratic regression. (C) Test of spatial TL for population density. Straight solid and curved dotted line are as in (B) for spatial variance and spatial mean. The curved dotted line is almost hidden by the straight solid line because the quadratic coefficient is very small and the other coefficients are almost identical to those of TL. Parameter estimates for linear and quadratic regressions in (B) and (C) are given in Table S1.

Fig. 2. The temporal TLs, temporal means and the temporal variances of population density in the Fundamental simulation (A, B, and C) and the Adjusted SD simulation (D, E, and F) (85 time series, each lasting 31 years). (A) Temporal TLs: $\log_{10}$(temporal variance) as a function of $\log_{10}$(temporal mean) for Fundamental simulations using observed $a_{1,j}$, observed $a_{2,j}$, and observed $SD_j$. (D) $\log_{10}$(temporal variance) as a function of $\log_{10}$(temporal mean) for Adjusted SD simulations using observed $a_{1,j}$, observed $a_{2,j}$, and adjusted $SD_j$. Solid line is the OLS regression for observed populations. The broken and dotted lines represent the linear and quadratic relationship in these simulations, respectively. (B and E) Simulated $\log_{10}$(temporal mean density) as a function of empirical $\log_{10}$(temporal mean density) in the Fundamental (B) and Adjusted SD (E) simulations. The solid line represents $y = x$. (C and F) Simulated $\log_{10}$(temporal variance of density) as a function of empirical $\log_{10}$(temporal variance of density) in the Fundamental (C) and Adjusted SD (F) simulations. The solid line represents $y = x$.

Fig. 3. The temporal (A, B, and C) and spatial (D, E, and F) TLs, means, and variances in 85 Synchronized $e_t$ simulations, each lasting 31 years, which were generated using observed $a_{1,j}$, observed $a_{2,j}$, and synchronized $e_{t,j}$. (A) The $\log_{10}$(temporal variance) as a function of $\log_{10}$(temporal

mean) for the simulated populations. The solid line is the OLS regression for the observed populations. The broken and dotted lines represent the linear and quadratic relationship in the simulations, respectively. (B) The $\log_{10}$(temporal mean) of the Synchronized $e_t$ simulations as a function of the $\log_{10}$(temporal mean) of the observed populations. The solid line represents $y = x$. (C) The relationship of $\log_{10}$(temporal variance) between the observed populations and the Synchronized $e_t$ simulations. The solid line represents $y = x$. (D) The $\log_{10}$(spatial variance) as a function of $\log_{10}$(spatial mean) for the simulated populations. The solid line is the OLS regression for the observed populations. The broken and dotted lines represent the linear and quadratic relationship in the simulations, respectively. (E) The relationship of $\log_{10}$(spatial mean) between the observed populations and the Synchronized $e_t$ simulations. The solid line represents $y = x$. (F) The relationship of $\log_{10}$(spatial variance) between the observed populations and the Synchronized $e_t$ simulations. The solid line represents $y = x$.

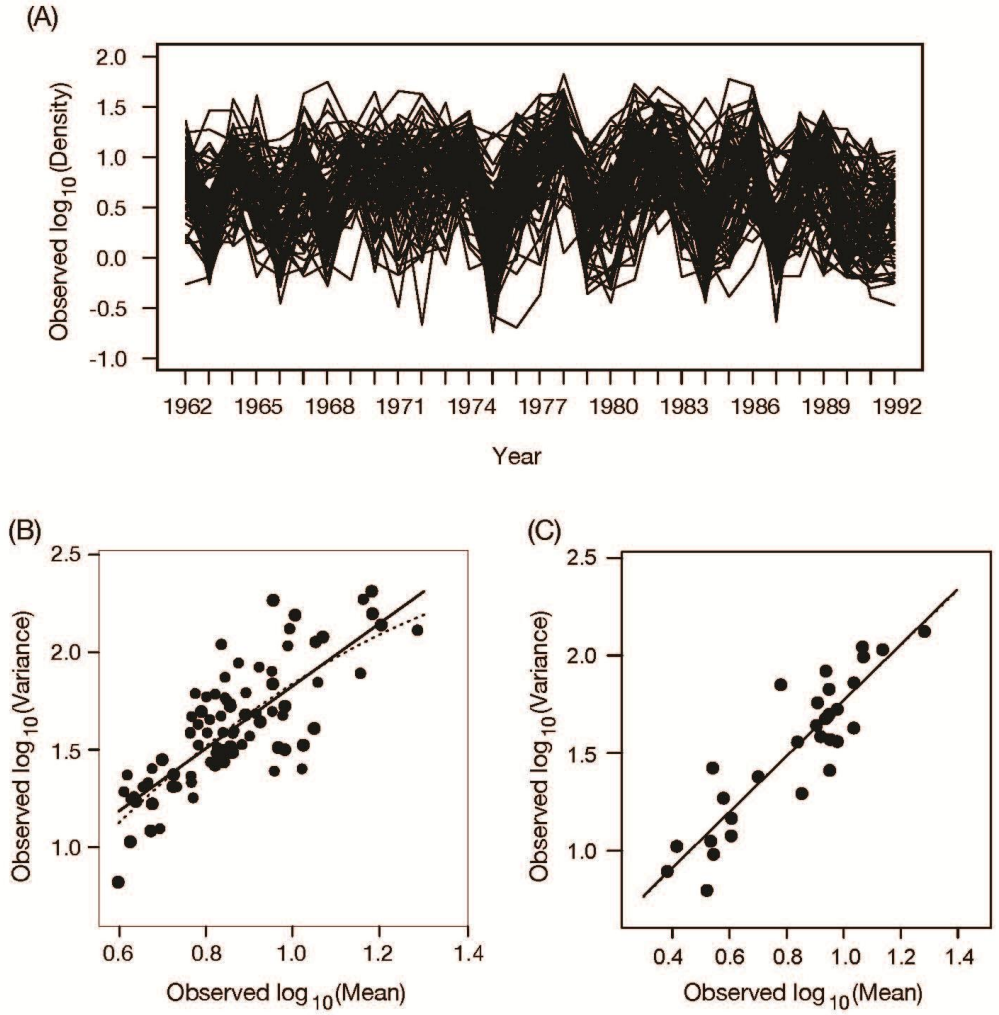


Figure 1

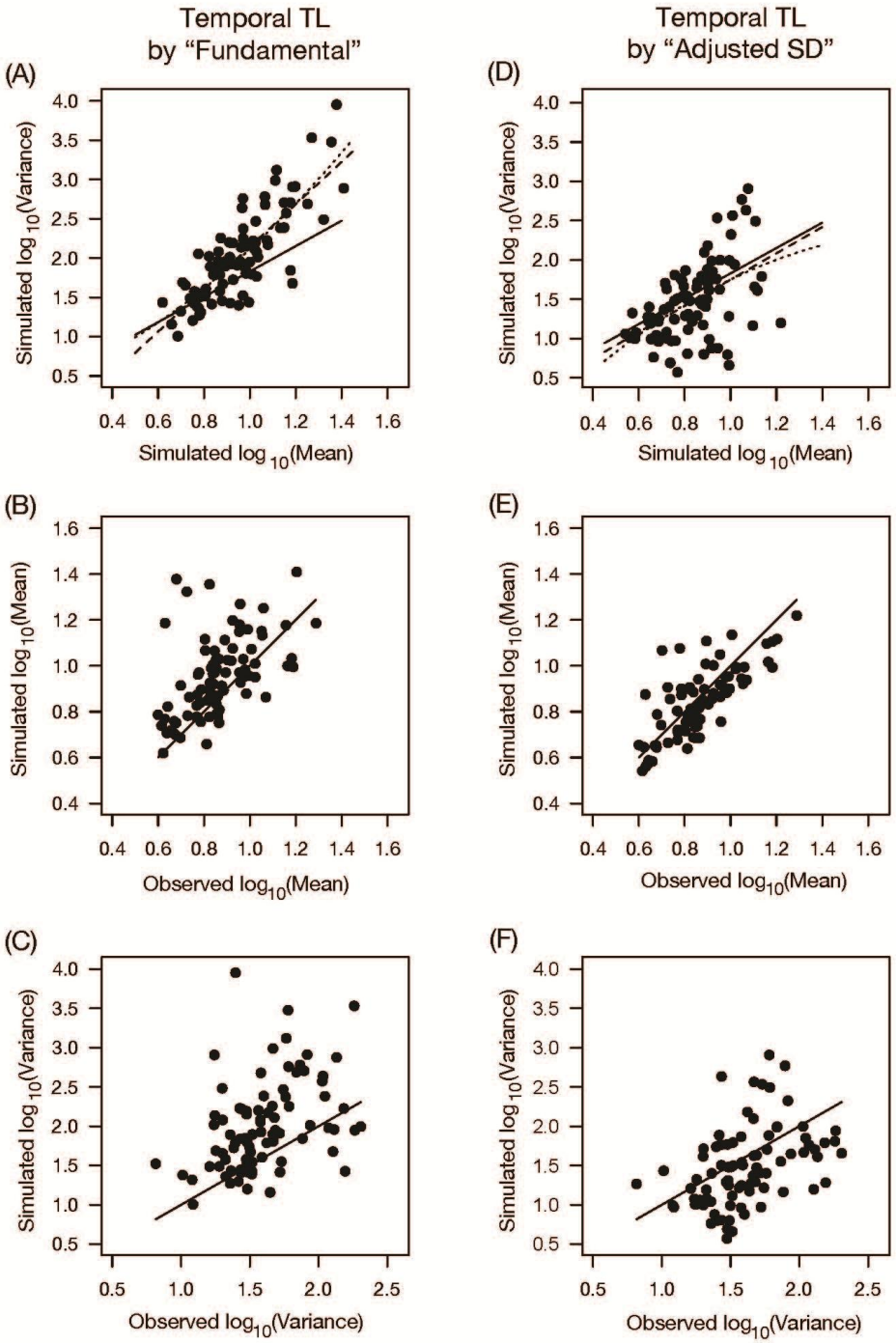


Figure 2

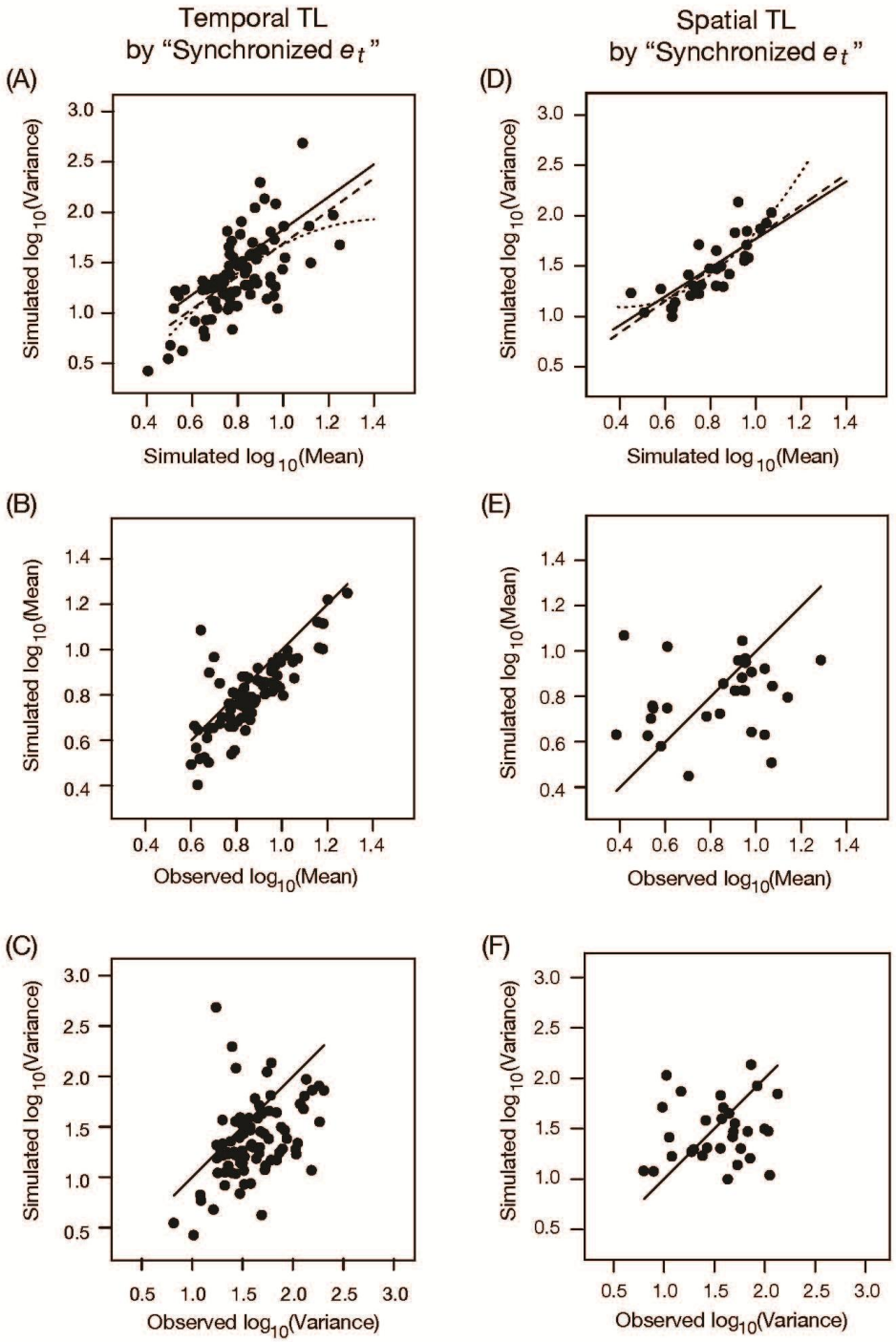


Figure 3